An Aerodynamic Theory Based on Time-Domain Aeroacoustics

Lyle N. Long*
Lockheed-California Company, Burbank, California

The aerodynamics of propellers and rotors is especially complicated because of the highly three-dimensional and compressible nature of the flowfield. However, when linearized theory is applicable, the problem is governed by the wave equation, and a numerically efficient integral formulation can be derived. This reduces the problem from one in space to one over a surface. Many such formulations exist in the aeroacoustics literature, but these become singular integral equations if one naively tries to use them to predict surface pressures, i.e., for aerodynamics. The present paper illustrates how one must interpret these equations in order to obtain nonambiguous results. After the regularized form of the integral equation is derived, a method for solving it numerically is described. Numerical results are compared to experimental results for ellipsoids, wings, and rotors, including effects due to lift.

Nomenclature

c = speed of sound
c_p = pressure coefficient $P/(\rho_0 V^2/2)$
$f(\bar{x},t)$ = description of body surface
$f_\epsilon(\bar{x},t)$ = ϵ region of body surface
$H(f)$ = Heaviside function
K_R = regular kernel
K_S = singular kernel
M = Mach number
M_n = $\bar{V}\cdot\hat{n}/c$, Mach number in normal direction
M_r = $\bar{v}\cdot\hat{r}/c$, Mach number in propagation direction
M_r = $(\partial\bar{M}/\partial\tau)\cdot\hat{r}$ derivative of Mach number in propagation direction
M_t = $\sqrt{M^2-M_n^2}$, Mach number in tangential direction
$\hat{n}$ = unit normal vector
P = perturbation pressure
r = $|\bar{r}|$
$\bar{r}$ = $\bar{x}-\bar{y}(\tau)$ = vector distance between source and observer
$\hat{r}$ = $\bar{r}/r$
R,R' = radial distance on body surface
ret = expression is evaluated at retarded time, $\tau=t-r/c$
t = time
v_r = $\bar{v}\cdot\hat{r}$, surface velocity in propagation direction
v_n = normal velocity of body
$\bar{v}$ = velocity of body
$\bar{x}$ = location of observer (stationary)
$\bar{x}_0$ = location of observation point, $\bar{x}$, when it is on the body at time $t=0$
$\bar{y}$ = $\bar{y}(\tau)$ = location of source (in motion)
β = $\sqrt{1-M^2}$
β_n = $\sqrt{1-M_n^2}$
β_t = $\sqrt{1-M_t^2}$
γ = angle on surface in ϵ region
δ = distance of source from body in normal direction
$\delta(f)$ = Dirac delta function
ϵ = size of hole removed from integral
θ = $\arccos(\hat{n}\cdot\hat{r})$
ρ = perturbation density
τ = $t-r/c$ = retarded time
ϕ = angle used in ϵ region
ω = angular velocity of body
Ω_r = $(\bar{\omega}\times\hat{n})\cdot\hat{r}$

Presented as Paper 83-1821 at the AIAA Applied Aerodynamics Conference, Danvers, Mass., July 13-15, 1983; submitted Sept. 17, 1983; revision received Aug. 20, 1984.

*Senior Aerodynamics Engineer. Member AIAA.

Introduction

THE present study was originally motivated by a need for effective noise prediction methods for moving bodies, especially rotating blades. There are several formulations for the noise due to moving bodies,[1] but they all require detailed surface pressure data. This is because the governing partial differential equations and boundary conditions are usually reduced to integral formulations using Green's function.

The present work will show that the surface pressure, or aerodynamics, can be calculated from the same integral formulations that govern the acoustics. Although in this case, instead of having an integral *representation*, one obtains an integral *equation*; specifically it will be a singular, inhomogeneous Fredholm integral equation of the second kind.

The key word is singular. Without this complication, there would be few difficulties. This is because singular integral equations are ambiguous unless interpreted properly. This interpretation forms much of this paper. In fact, the main result of the present work was to derive the form of the equation on the surface and to solve it using a time-domain panel method for several different bodies.

Using the acoustic analogy approach implies that he pressure (or density) will be the dependent variable. A major advantage in using this formulation as opposed to using the velocity potential is that there is no need to integrate over the wake. Since the pressure, unlike the velocity potential, is continuous across the wake, there will be no integrals over the surface of the wake.

It is well known that linearized acoustics and linearized compressible aerodynamics are one and the same. They both derive from a small perturbation of the continuity and Euler equations, which can be combined to give the wave equation. Generally, acoustics is concerned with the signal after it has radiated from the body. Aerodynamics is concerned with determining the forces on the body. In the current work both effects will be shown to originate from the same phenomenon. Just as one can find the pressure on a vibrating piston using the Kirchhoff-Helmholtz equation,[2] the pressure on any thin or slender body can be determined using Farassat's equation.

Linearized compressible aerodynamics is governed by the wave equation, for steady, rectilinear motion the problem is known to be simplified considerably. Using the Prandtl-Glauert transformation the wave equation can be transformed into the Laplace equation, allowing one to use the well-known and powerful methods of potential theory. For finite bodies

undergoing complicated motions such as spinning, vibrating, and translating, the problem is not so simple. One has no alternative but to solve the wave equation. The method presented herein represents a solution technique for the wave equation. Compressibility, three-dimensionality, and complicated motions are treated together in a unified fashion. Once one becomes accustomed to the notion of four dimensions, the physics become much more understandable.

Compressibility manifests itself via a finite propagation speed of disturbances. This is exactly how compressibility effects are accounted for in this work. The time of propagation is calculated. In rectilinear motion this is equivalent to the Prandtl-Glauert transformation, where the body is "stretched" in order to account for the actual distance the signal travels. Because the body and the signal are moving, the signal must travel further in order to go from one point on the body to another. Compressibility will be discussed later in terms of retarded time, which has also been used by several authors.[3-9] After the integral equation governing the surface pressure is derived, the numerical technique used to solve it will be discussed.

The numerical approach used here can be classified as a boundary integral equation (BIE) method or panel method.[10] Numerous very effective panel methods exist for steady flow, notably PANAIR[11] and QUADPAN,[12] which were developed by Boeing and Lockheed, respectively. Panel methods have been very effective for aircraft configurations, but they are not suitable for rotating blades because they use two-dimensional or rectilinear compressibility corrections (Prandtl-Glauert, Gothert, or Karman-Tsien rules[13]).

The current work is based on the linearized Ffowcs Williams-Hawkings (FW-H) equation[14]:

$$\bar{\Box}^2 p = \frac{\bar{\partial}}{\partial t}[\rho_0 v_n \,|\nabla f|\,\delta(f)] - \frac{\bar{\partial}}{\partial x_i}[p n_i \,|\nabla f|\,\delta(f)] \qquad (1)$$

where $\Box^2$ signifies the wave operator,

$$\Box^2 p = \frac{1}{c^2}\frac{\partial^2 p}{\partial t^2} - \nabla^2 p$$

Equation (1) represents a combination of the conservation of mass and momentum equations, plus the boundary conditions. The forcing terms are zero everywhere but on the surface of the body, $f=0$.

Farassat has derived several different integral representations of the above equation. Each one is particularly well-suited to a different application or numerical solution technique. The one that is most appropriate for the present work is Eq. (9) of Ref. 5:

$$4\pi p(\boldsymbol{x},t) = \frac{1}{c}\frac{\partial}{\partial t}\int_{f=0}\left(\frac{\rho_0 c v_n + p\cos\theta}{r\,|1-M_r|}\right)_{\text{ret}} \mathrm{d}s + \int_{f=0}\left(\frac{p\cos\theta}{r^2\,|1-M_r|}\right)_{\text{ret}} \mathrm{d}s \qquad (2)$$

If one knows the surface pressure on a given body this equation will predict the noise due to that body. The subscript "ret" signifies that the expression is to be evaluated at retarded time. This accounts for the fact that the "source" at $\bar{y}(\tau)$ (in motion) emits a signal that arrives at the stationary "observer" at $\bar{x}$ a short time after it is emitted. This is unlike incompressible flow where signals travel with infinite speed. Therefore, the integration over the body surface, $f(\bar{x},t)=0$, is not carried out at a single emission time τ, because different points on the surface have different emission times.

Equation (2) represents the starting point for this paper. Although it has been effective in predicting noise from bodies in motion, it has not been used to predict surface pressures on arbitrary bodies, mainly because the integrals become singular when the observer is on the surface. A mathematical limiting procedure is required, the details of which are described in the next section.

Farassat's Eq. (2) is an integrodifferential equation. Taking the derivative inside the integral will produce an additional singular integrand, i.e., one with $1/r^2$ dependence. Since the main interest here is in the form of the equation on the surface, it is important to bring the derivative under the integral sign. This will illuminate the singular term and allow it to be regularized. This has been done by Farassat[15] and Long[16]:

$$4\pi p(\boldsymbol{x},t) = \int_{f=0} K_R(\boldsymbol{x},t;\boldsymbol{y},\tau)\,\mathrm{d}S + \int_{f=0} K_S(\boldsymbol{x},t;\boldsymbol{y},\tau)\,\mathrm{d}S \qquad (3)$$

where

$$K_R = \left\{\frac{\rho_0 c^2 M_n \dot{M}_r + p\Omega_r(1-M_r) + p\dot{M}_r\cos\theta}{cr(1-M_r)^3}\right\}_{\text{ret}}$$

$$K_S = \left\{\frac{\rho_0 c^2 M_n (M_r - M^2) + p[(1-M^2)\cos\theta - (1-M_r)M_n]}{r^2(1-M_r)^3}\right\}_{\text{ret}}$$

Analysis

Singular Integrals and Boundary Solutions

Singular integrals are very common in mathematical physics, especially aerodynamics, because of the frequent use of the Green's function technique. Whenever one desires surface information from such a method, singular integrals may arise. Usually, however, these integrals are special cases of regular integrals, and their proper interpretation can be inferred from the physics.

The proper way to interpret singular integrals is through a limiting process.[16-20] In the acoustic formulations, one must assume the observer goes to the surface in the limit. However, this limit must be taken after integrating over the surface, which presents a problem for complicated integrals such as are present here.

Integral Equation Valid on Body Surface

In this section a procedure equivalent to Mangler's[20] will be applied to Farassat's equation in order to obtain an equation valid on the surface of the body. It will be semiconvergent and the form of the "extra" term that comes from the ϵ region will depend upon the size and shape of the ϵ region just as for the downwash integral of the Cauchy principal value.[16]

The first step in interpreting Eq. (3) is to divide the region of integration into two parts—one that includes the singularity and one that does not. In the case of the downwash integral this was done by breaking the ξ axis into three different parts.[16] Farassat's equation is an integral over a surface, so the surface will be divided into two parts. One part will be over the original body surface with a small hole around the

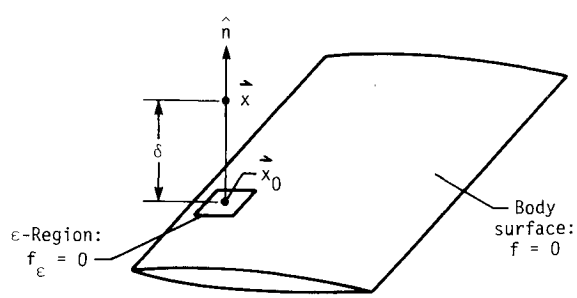

Fig. 1 ϵ region of arbitrary body.

singularity removed; the other part will be the surface of the hole itself. See Fig. 1.

The combination of these two regions is the original surface $f(\bar{x},t)=0$. Thus, Eq. (3) is written

$$4\pi p(\mathbf{x},t)=\int_{f=0} K_R(\mathbf{x},t;\mathbf{y},\tau)\mathrm{d}S+\oint\!\!\!\!\!\!\diagup_{f=0} K_S(\mathbf{x},t;\mathbf{y},\tau)\mathrm{d}S$$
$$+\int_{f_\epsilon=0} K_s(\mathbf{x},t;\mathbf{y},\tau)\mathrm{d}S \tag{4}$$

where $\oint\!\!\!\!\!\!\diagup$ indicates that a specific hole has been removed and f_ϵ is the surface of the hole. Note that it is not necessary to break up the region of integration in the regular integral K_R.

The first two integrals above will produce no difficulties numerically since they are both convergent. By definition, neither of them contains a singularity. The third integral is difficult to calculate numerically. The proper way to obtain its form, at $\bar{x}_0$, is via a mathematical limiting process where the observer is located at $\bar{x}$ a distance of δ above the surface. Then, after integrating, the limit as $\delta\to 0$ is performed. (See Fig. 1.) This is analogous to taking the limit as $y\to 0$ in the downwash integral. Note that for convenience $\bar{x}$ is taken to be along the normal to the surface at $\bar{x}_0$. Mathematically one can write the procedure as

$$p(\mathbf{x}_0,t)=\lim_{\delta\to 0} p(\mathbf{x},t)$$

Hence the above integral equation becomes

$$4\pi p(\mathbf{x}_0,t)=\int_{f=0} K_r(\mathbf{x}_0,t;\mathbf{y},\tau)\mathrm{d}S+\oint\!\!\!\!\!\!\diagup_{f=0} K_S(\mathbf{x}_0,t;\mathbf{y},\tau)\mathrm{d}S$$
$$+\lim_{\delta\to 0}\int_{f_\epsilon=0} K_S(\mathbf{x},t;\mathbf{y},\tau)\mathrm{d}S \tag{5}$$

The first two integrals are obtained by simply replacing $\bar{x}$ by $\bar{x}_0$ (setting $\delta=0$). This is valid since they are convergent, but it is not possible in the third integral. One has no alternative but to perform that integration *first* and then take the limit—otherwise the integral is divergent. The problem with this is that this integral is too complicated to allow analytic evaluation for most bodies of interest, especially since the integrand K_S contains the unknown pressure P. One would have to solve the entire integral equation and then take the limit as $\delta\to 0$. This would give an analytic expression for the surface pressure.

By assuming that the size of the hole or ϵ region is small, one can approximate the region as planar. In addition, the pressure can be expanded in a Taylor series about the point $\bar{x}_0$, which is equivalent to assuming it is constant over the ϵ region. Using these approximations one can then calculate the third integral in Eq. (5) analytically and obtain an estimate of the error involved. The remainder of this section will be devoted to obtaining the appropriate analytic expression for the third integral in Eq. (5).

In order to perform this integration over a small square-planar panel, one must first write the integrand K_S in terms of surface coordinates. Figure 2 is an enlarged view of the ϵ region shown in Fig. 1. It shows the panel at two different times. The time t is the reception time and τ is the emission time. Thus, a signal emitted from the surface point $\bar{y}(\tau)$ at time τ is received at the (stationary) observer point $\bar{x}$ at time t. The δ on this figure is the same δ that was used on Fig. 1. The upper plane is the position of the panel at time t, the time when the observer receives the signal from $\bar{y}(\tau)$. The lower plane is the position of the panel when the signal was emitted. The angle between the surface normal $\hat{n}$ and the radiation direction $\hat{r}$ is called θ. For convenience, the coordinate system (fixed to the panel) is aligned so that the panel velocity vector is in the y-z plane. The angle between the velocity and the z axis is defined as Φ.

As mentioned earlier, the observation point $\bar{x}$ is always stationary. Therefore, when one speaks of the observation point being "on" the surface, one must specify at what time this occurs. In Fig. 2, notice that the position $\bar{x}$ will go to $\bar{x}_0(t)$ when $\delta\to 0$. This surface point $\bar{x}_0$ is, of course, moving, but when the time equals t it is a distance δ away from $\bar{x}$ in the direction of the normal. This means $|\bar{x}-\bar{x}_0(t)|=\delta$.

Figure 2 is useful because many of the quantities on it are known. For example, it is known that $r=c(t-\tau)$ since the distance a signal travels is simply the speed multiplied by the time of propagation. In addition, the distance the panel moves in this time period is $|\bar{x}_0(\tau)-\bar{x}_0(t)|$, which is $v(t-\tau)$. This means $rM=v(t-\tau)$.

The purpose of this section is to integrate K_S over the area of this arbitrary panel. By assuming a planar panel, one can simplify K_S considerably. For example, it is obvious that

$$\cos\theta=M_n+\delta/r$$

where $M_n=\bar{v}\cdot\hat{n}/c$. This means Eq. (5) can be written as

$$4\pi p(\mathbf{x}_0,t)=\int_{f=0} K_R\mathrm{d}S+\oint\!\!\!\!\!\!\diagup_{f=0} K_S\mathrm{d}S$$
$$+M_n(\rho_0c^2+p)\lim_{\delta\to 0}\int_{-\epsilon}^{\epsilon}\int_{-\epsilon}^{\epsilon}\left[\frac{M_r-M^2}{r^2(1-M_r)^3}\right]_{\mathrm{ret}}\mathrm{d}y_1\mathrm{d}y_2$$
$$+p\lim_{\delta\to 0}\int_{-\epsilon}^{\epsilon}\int_{-\epsilon}^{\epsilon}\left[\frac{\beta^2\delta}{r^3(1-M_r)^3}\right]_{\mathrm{ret}}\mathrm{d}y_1\mathrm{d}y_2+\mathcal{O}(\epsilon) \tag{6}$$

where P and $\bar{v}$ have been expanded in a Taylor series about $\bar{y}=\bar{x}_0$.

All that is required now in order to integrate the above is to write the integrands in the last two integrals in terms of y_1 and y_2. This is relatively easy to do using the geometry shown in Fig. 2. The propagation vector $\bar{r}$ can be written in terms of its components in the local coordinate system shown in Fig. 2.

$$\bar{r}=(R\sin\gamma, rM_t-R\cos\gamma, \delta+rM_n) \tag{7}$$

Therefore the magnitude of $|\bar{r}|=r$ is governed by

$$\beta^2r^2+2(RM_t\cos\gamma-\delta M_n)r-R^2-\delta^2=0$$

where $\beta^2=1-M^2$ and $M^2=M_n^2+M_t^2$.

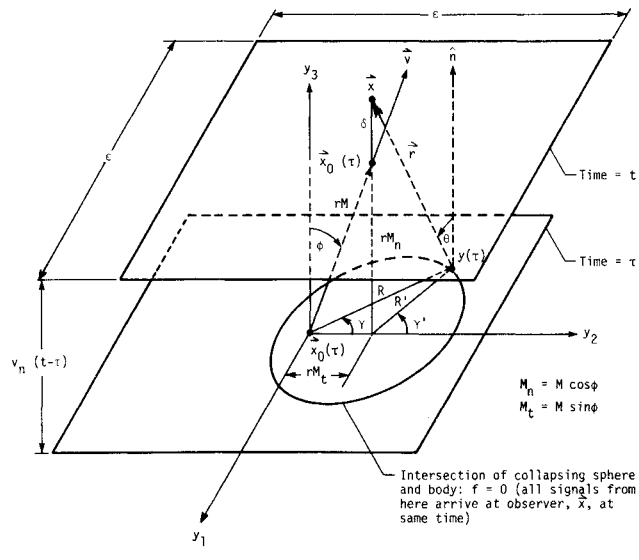

Fig. 2 Geometry near singularity in retarded time.

Using the quadratic formula gives

$$\beta^2 r = (\delta M_n - RM_t\cos\gamma) + \sqrt{(\delta M_n - RM_t\cos\gamma)^2 + \beta^2(R^2+\delta^2)} \tag{8}$$

This can be written in a simpler form by taking the scalar product of the Mach number vector $M=(0,M_t,M_n)$ and $\bar{r}$ [Eq. (7)] to get

$$rM_r = M^2 r - RM_t\cos\gamma + \delta M_n \tag{9}$$

Now Eqs. (8) and (9) can be combined to give

$$r(1-M_r) = \sqrt{\beta^2R^2 + R^2M_t^2\cos^2\gamma - 2RM_t\delta M_n\cos\gamma + \beta_t^2\delta^2}$$

where

$$\beta_t^2 = 1 - M_t^2$$

Changing to Cartesian coordinates, where $R^2 = y_1^2 + y_2^2$ and $R\cos\gamma = y_2$ gives

$$r(1-M_r) = \sqrt{\beta^2 y_1^2 + \beta_n^2 y_2^2 - 2M_tM_n\delta y_2 + \beta_t^2\delta^2} \tag{10}$$

This is now in a form that will allow the analytic integration of Eq. (6). It remains to write $M_r - M^2$ in terms of y_1 and y_2. This can be obtained from Eq. (9) in the form

$$M_r - M^2 - (\delta M_n - y_2 M_t)/r \tag{11}$$

Using Eqs. (10) and (11) in Eq. (6) gives, after simplifying,

$$4\pi p(x_0,t) = \int_{f=0} K_R\,dS + \oint_{f=0} K_S\,dS + (\rho_0 v_n^2 + \beta_t^2 p)$$
$$\times \lim_{\delta\to 0} \int_{-\epsilon}^{\epsilon}\int_{-\epsilon}^{\epsilon} \frac{\delta\,dy_1\,dy_2}{(\beta^2y_1^2 + \beta_n^2y_2^2 - 2\delta M_nM_ty_2 + \beta_t^2\delta^2)^{3/2}}$$
$$-M_nM_t(\rho_0c^2 + p)$$
$$\times \lim_{\delta\to 0} \int_{-\epsilon}^{\epsilon}\int_{-\epsilon}^{\epsilon} \frac{y_2\,dy_1\,dy_2}{(\beta^2y_1^2 + \beta_n^2y_2^2 - 2\delta M_nM_ty_2 + \beta_t^2\delta^2)^{3/2}} + \mathcal{O}(\epsilon)$$

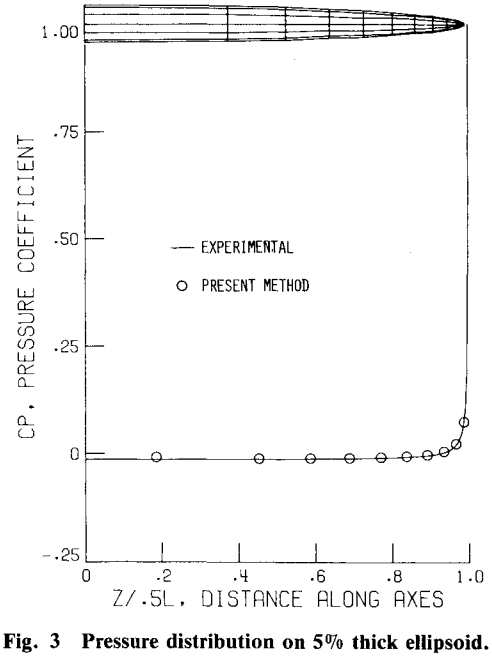

Fig. 3 Pressure distribution on 5% thick ellipsoid.

where $r(1-M_r)$ is given by Eq. (10). These can be integrated using transformations of the form

$$\eta = \beta_n^2 y_2 - M_nM_t\delta \qquad \xi = \beta\beta_n y_1$$

which is described in detail in Ref. 16. The final result is:

$$4\pi p(\bar{x}_0,t) = \int_{f=0} K_R\,dS + \oint_{f=0} K_S\,dS$$
$$+\frac{2}{\beta_n^2}(\rho_0 v_n^2 + p)\lim_{\delta\to 0}\left\{\frac{\delta\eta_2}{|\delta\eta_2|}\tan^{-1}\left[\left|\frac{\eta_2}{\delta}\right|\frac{\beta_n\epsilon}{\Gamma_2}\right]\right.$$
$$\left.-\frac{\delta\eta_1}{|\delta\eta_1|}\tan^{-1}\left[\left|\frac{\eta_1}{\delta}\right|\frac{\beta_n\epsilon}{\Gamma_1}\right]\right\}$$
$$+\frac{2M_nM_t}{\beta\beta_n^2}(\rho_0c^2 + p)\lim_{\delta\to 0}\left\{\ell n\left[\frac{\Gamma_2 + \beta\beta_n\epsilon}{\Gamma_1 + \beta\beta_n\epsilon}\right]\right.$$
$$\left.-\ell n\left[\frac{\sqrt{\eta_2^2 + \beta^2\delta^2}}{\sqrt{\eta_1^2 + \beta^2\delta^2}}\right]\right\} + \mathcal{O}(\epsilon) \tag{12}$$

where

$$\Gamma_1 = \sqrt{\eta_1^2 + \beta^2\beta_n^2\epsilon^2 + \beta^2\delta^2}$$
$$\Gamma_2 = \sqrt{\eta_2^2 + \beta^2\beta_n^2\epsilon^2 + \beta^2\delta^2}$$
$$\eta_1 = -\beta_n^2\epsilon - M_nM_t\delta, \quad \eta_2 = \beta_n^2\epsilon - M_nM_t\delta, \quad \xi_2 = \beta\beta_n\epsilon$$

Notice that, for incompressible flow, this is similar to Eq. (5-82) of Ref. 21. Taking the limit, Eq. (12) becomes simply

$$4\pi\left(1 - \frac{1}{2\beta_n^2}\right)p(x_0,t) = \int_{f=0} K_R\,dS + \oint_{f=0} K_S\,dS$$
$$+\frac{2\pi\rho_0 v_n^2(x_0,t)}{\beta_n^2} + \mathcal{O}(\epsilon) \tag{13}$$

The above equation represents the governing equation—amenable now to numerical techniques—for the pressure on a body in compressible, subsonic motion. The theory is linearized so that it is expected to be more and more accurate for thin or slender bodies, which includes most bodies of aerodynamic interest. Note that Eq. (13) is applicable to the outside of the body. The coefficients are slightly different in the equation governing the pressure inside the body, as described in Ref. 16.

Lifting Bodies

Determining the surface pressure on lifting bodies is, of course, much more difficult than on nonlifting bodies because lift is an inherently viscous effect. To approximate viscous effects using an inviscid theory, one must obviously use not only physics but experimental results in order to extend the theory.

The linearized, inviscid equations used herein neglect several important features of the actual flow. First, the flow is assumed to slip over the body, which means that no tangential velocity boundary condition is prescribed. This immediately leads to a question of uniqueness, for there are an infinite number of velocity fields that satisfy the normal velocity boundary condition. The Kutta or trailing edge condition is usually used to determine which of these velocity fields is appropriate, since it is known that viscosity will prevent the flow from turning the sharp angle at the trailing edge.

Another difficulty in using the FW-H equation to predict lift is that there is no built-in mechanism to generate lift. The circulation is assumed to be zero. The well-known panel methods distribute vortices or doublets on or inside the body, where their strengths are determined by satisfying a Kutta con-

dition. These simply provide a means of altering the onset flow. Instead of having only uniform mean flow, these provide a circulatory contribution to the onset flow also. Of course, one must still satisfy the normal velocity boundary condition. Using the FW-H equation with stagnation flow inside the body means there is no simple way to include vorticity. However, there is a way to condition the final system of linear equations and obtain the effects due to lift. This will be accomplished without using the concept of vortices distributed on the body. More detailed discussions of the lifting problem are contained in Ref. 22.

In order to fully understand the technique used to condition the equations, one must consider what the flowfield is really like around a lifting airfoil. A major difference between a lifting and nonlifting airfoil is the location of the leading edge stagnation point. Conversely, the Kutta condition tells us that the trailing edge stagnation point is in the same location for lifting and nonlifting airfoils. All of this means that the trailing edge experiences essentially the same flow whether the body is at an angle of attack or not. This is basically what van Holten[6] implies when he advocates placing only the leading edge at an angle of attack. He uses the acceleration potential and finds that using this "variable-geometry" concept forces his inviscid results into close agreement with real lifting flows. Apparently, these ideas can be traced back to Lanchester.

However, van Holten's suggestion is not quite as practical as the means of applying the Kutta condition used herein. Reference 16 describes this technique and presents a simple example of its use. Basically, when using the pressure or acceleration-potential method one must set the pressure equal on the upper and lower surfaces of the trailing edge. This can be done quite easily by conditioning the forcing terms in the final system of algebraic equations. This conditioning just means replacing the terms corresponding to the panels on the upper and lower surface at the trailing edge by the average of the two values. This effectively forces the flow to be symmetric over the aft portion of the airfoil, with the stagnation point at the trailing edge.

Computational Method

Since the purpose of the numerical procedure in the present work was to verify the feasibility of the method and not to develop a production computer program, it seemed appropriate to solve the equation directly rather than to introduce additional complications. Therefore, the computer program that was developed simply uses Legendre-Gaussian quadrature. Of course, more efficient or sophisticated methods may be developed later on.

In order to improve efficiency, the computer program calculates the number of nodes to use for each integration. When the observer and source panels are very close together, the integrand varies rapidly, which means a large number of quadrature points are required. Conversely, when the source and observer panels are far apart just a few points may be required. The program currently uses between 1 and 64 quadrature points for each integration. A more detailed description of how the number of points is determined is given in Ref. 16. The program also calculates the retarded-time distance between the source and the observer, which is governed by a simple transcendental equation. A Newton-Raphson technique is used to determine this distance.[16]

Results

This section presents numerical results for several different types of bodies in various combinations of rectilinear and angular motion. Using the computer program described in the previous section, the surface pressure was calculated for prolate ellipsoids, wings, and rotating blades. These different types of bodies were used to illustrate the generality of the method.

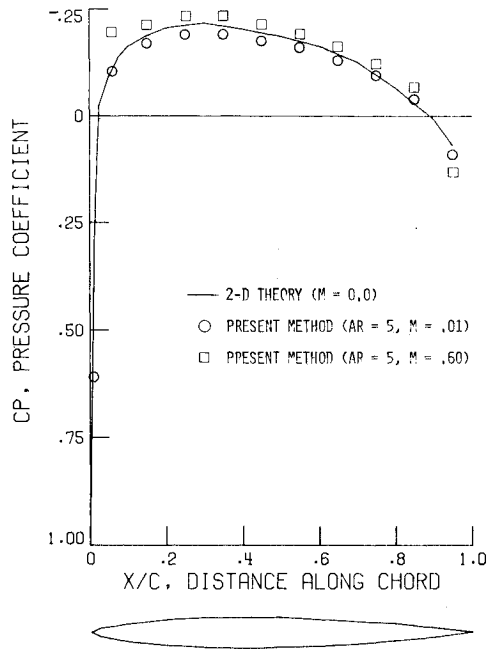

Fig. 4 Pressure distribution on an NACA 0008 wing.

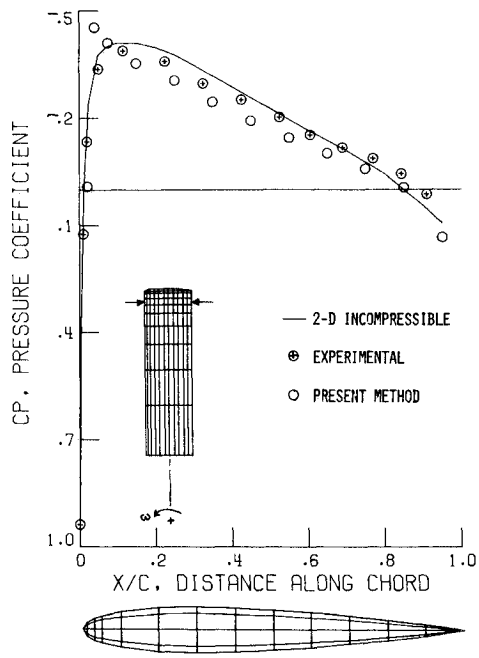

Fig. 5 Pressure distribution on an NACA 0012 rotor at 90% span, $\alpha = 0$ deg.

Prolate Ellipsoids

A prolate ellipsoid with a fineness ratio of 0.05 was modeled in low-speed motion. This was chosen because of the availability of theoretical (incompressible) and experimental results with which to compare.[23] The ellipsoid was modeled using 264 panels.

The numerical and experimental results are also compared in Fig. 3, which is a graph of pressure coefficient vs axial distance. The solid line represents experimental results,[23] and the symbols represent the current results. Agreement is generally good, except near the stagnation point where one of the points is off the scale, but this is expected because of the use of linearized theory.

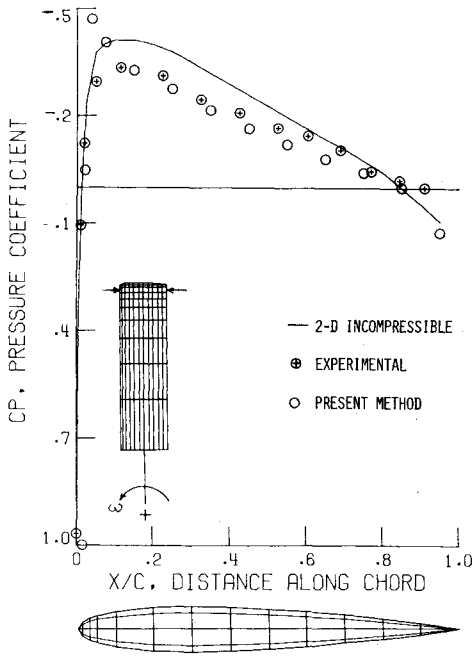

Fig. 6 Pressure distribution on an NACA 0012 rotor at 98% span, $\alpha = 0$ deg, $M_{TIP} = 0.25$.

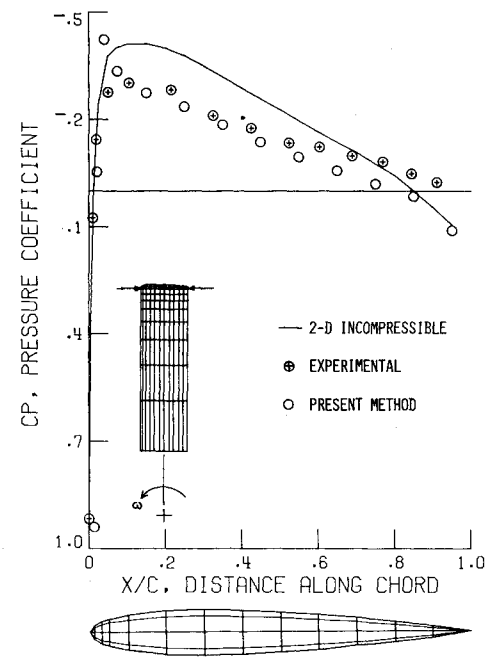

Fig. 7 Pressure distribution on an NACA 0012 rotor at 99.5% span, $\alpha = 0$ deg, $M_{TIP} = 0.25$.

Near the ends of the ellipsoid the flow is essentially that for a blunt body. Linearized theory is usually valid to within a few percent of the chord from the leading edge.[21] For more detailed descriptions of the flow near the stagnation point one could use the methods of Van Dyke[24] or include the quadrupole terms in the present formulation—which includes the nonlinear terms. Neither of these would be trivial to incorporate into the current scheme. Reference 16 presents similar results for thicker ellipsoids.

Finite Wing

The next example is that of a finite wing with an NACA 0008 cross section and an aspect ratio of 5. There were 242 panels with no special precautions taken near the tip. In fact, the tips are not paneled at all—they are actually open. Including these panels had an insignificant effect on the panels away from the tips. And since this section will be comparing numerical results to two-dimensional section airfoil theory, only results from the center of this finite wing will be shown.

The numerical results are presented in Fig. 4. Also shown are two-dimensional potential theory results (incompressible).[25] The numerical results were obtained for Mach numbers of 0.01 and 0.6, and compare very well with the theoretical results. Correcting the two-dimensional incompressible results using the Prandtl-Glauert rule would produce a curve slightly above the $M = 0.6$ data points. The finite aspect ratio may account for the numerical results being slightly lower than the theoretical.

Helicopter Rotor Blade

In this section numerical results are presented for a rotating NACA 0012 blade. This airfoil section is common in helicopter applications. The results will be compared to the experiments of Gray.[26] The blade was approximated by 264 finite panels. Panel sizes were decreased smoothly from root to tip. Blade length was 6.5 chord lengths. Tip Mach number was 0.25 and there was zero angle of attack.

Figs. 5-7 compare the variation in the pressure coefficient along the chord for three spanwise locations: 94, 98, and 99.5%. The solid line represents two-dimensional airfoil theory.[24] The circular symbols are experimental results[25] and the squares are the present numerical calculations. These

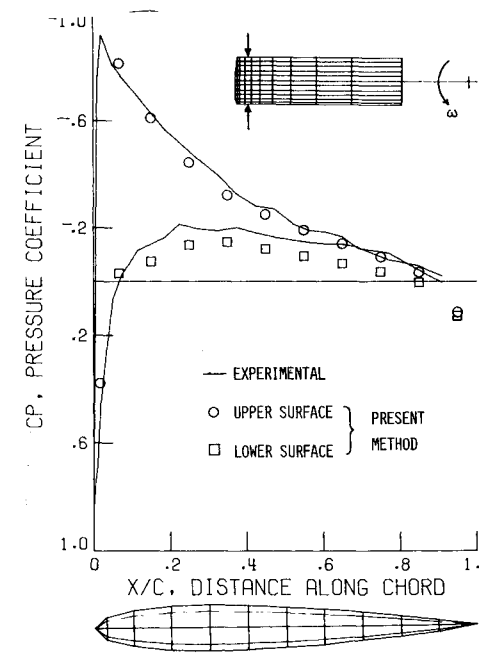

Fig. 8 Pressure distribution on an NACA 0012 rotor at 94% span, $\alpha = 6.18$ deg, $M_{TIP} = 0.25$.

results indicate good agreement with experiment. Notice how close to the two-dimensional theory the results are at the 94% span location. The three-dimensional effects are obvious as one moves closer to the tip. Of course at the leading edge the well-known square-root singularity appears.

Figures 8-10 present similar results for the blade at an angle of attack. Using the concepts discussed earlier allows the calculation of surface pressures on lifting bodies. As described there, the inhomogeneous terms of the system of algebraic equations must be "conditioned." This conditioning consists of replacing the inhomogeneous terms (for the panels on the upper and lower surfaces at the trailing edge) by the average of the two values. This must be done for all panels from the trailing edge to the thickest part of the cross section.

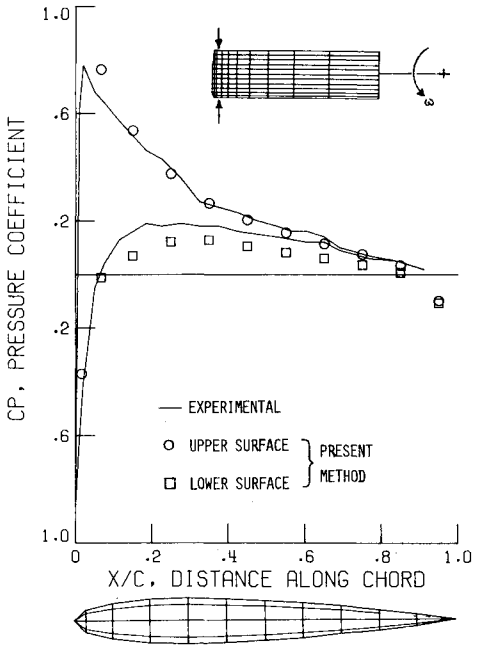

Fig. 9 Pressure distribution on an NACA 0012 rotor at 98% span, $\alpha = 6.18$ deg, $M_{TIP} = 0.25$.

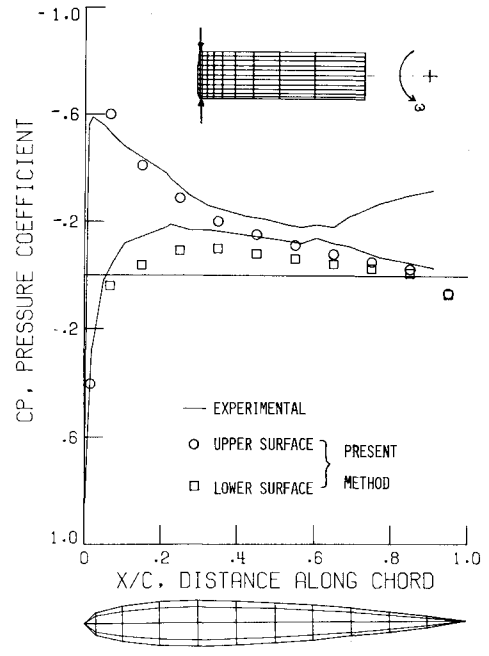

Fig. 10 Pressure distribution on an NACA 0012 rotor at 99.5% span, $\alpha = 6.18$ deg, $M_{TIP} = 0.25$.

Conclusion

This paper describes a method for calculating the surface pressure on arbitrary bodies in compressible flow. It is based on the acoustic analogy approach of Ffowcs Williams and Hawkings, and an equation due to Farassat. Its major contributions have been in interpreting Farassat's equation when the observation point is located on the surface of the body and in solving the resulting equation numerically.

Since Farassat's equation is based on linearized, inviscid theory, the method presented here will of course have its limitations. These have been pointed out whenever possible in the text. For bodies moving in rectilinear motion there may be more appropriate theories to use, since one is then able to include some of the nonlinear effects relatively easily. On the contrary, for bodies such as propellers and helicopter rotors the present results are very encouraging because of the extreme complexity of the problem. The method is based on first principles and is relatively easy to comprehend, yet it provides an inexpensive way to obtain very useful information. In addition, because the Ffowcs Williams-Hawkings equation does contain viscous and nonlinear terms, there is hope for including these effects in the future.

The method described herein contains several ideas that are somewhat novel to aerodynamic theory. First, compressibility is accounted for exactly as it occurs in nature—in terms of retarded time. Compressibility manifests itself as a finite speed of propagation of disturbances, and in the current theory the distance the signal actually travels is calculated.

Acknowledgments

This work was sponsored by NASA Langley Research Center under Cooperative Agreement NCC1-14. It is based on the author's Doctor of Science dissertation submitted to The George Washington University. The support and encouragement of Dr. F. Farassat and Dr. M. K. Myers are gratefully acknowledged.

References

[1]Farassat, F., "Linear Acoustic Formulas for Calculation of Rotating Blade Noise," *AIAA Journal*, Vol. 19, No. 9, Sept. 1981, pp. 1122-1130.

[2]Pierce, A. D., *Acoustics: An Introduction to Its Physical Principles and Applications*, McGraw-Hill, New York, 1981.

[3]Kussner, H. G., "General Airfoil Theory," NACA TM 979, 1941.

[4]Kondo, K., "On the Potential-Theoretical Fundamentals of the Aerodynamics of Screw Propellers at High Speed," *Journal of Faculty of Engineers*, University of Tokyo, Vol. 25, No. 1, 1957, pp. 1-39.

[5]Farassat, F., "Theory of Noise Generation from Moving Bodies with an Application to Helicopter Rotors," NASA TR R-451, 1975.

[6]van Holten, Th., "The Computation of Aerodynamic Loads on Helicopter Blades in Forward Flight, Using the Method of the Acceleration Potential," Technische Hodgeschool Delft, Rept. VTH-189, 1975.

[7]Das, A., "Wave Propagation and Methods of Solution of the Wave Equation for Moving Disturbance Sources," NASA TM-77409, Feb. 1984; Technical Transaction of DFVLR-FB, Jan. 1983.

[8]Dat, R., "Lifting Surface Theory Applied to Fixed Wings and Propellers," European Space Agency Rept. ESRO-TT-90, 1973 (N75-10016).

[9]Morino, L., "A General Theory of Unsteady Compressible Potential Aerodynamics," NASA CR-2464, 1974.

[10]Cruse, T. A. and Rizzo, F. J., "Boundary Integral Equation Method: Computational Applications in Applied Mechanics," ASME, AMD Vol. 11, New York, 1975.

[11]Moran, J., Tinoco, E. N., and Forrester, T. J., "User Manual—Subsonic/Supersonic Advanced Panel Pilot Code," NASA CR-152407, 1978.

[12]Youngren, H. H., Bouchard, E. E., Coopersmith, R. M., and Miranda, L. R., "Comparison of Panel Method Formulations and Its Influence on the Development of QUADPAN, an Advanced Low-Order Method," AIAA 83-1827, 1983.

[13]Liepmann, H. W. and Roshko, A., *Elements of Gasdynamics*, Wiley, New York, 1957.

[14]Ffowcs Williams, J. E. and Hawkings, D. L., "Sound Generation by Turbulence and Surfaces in Arbitrary Motion," *Proceedings of Royal Society (London)*, Series A264, 1969, pp. 321-342.

[15]Farassat, F., "Advanced Theoretical Treatment of Propeller Noise," von Kármán Institute Lecture Series 81-82/10, May 1982.

[16]Long, L. N., "The Compressible Aerodynamics of Rotating Blades Based on an Acoustic Formulation," NASA TP-2197, Dec. 1983; D.Sc. Dissertation, George Washington University, Washington, D.C., April 1983.

[17]Morse, P. M. and Feshbach, H., *Methods of Theoretical Physics*, McGraw-Hill, New York, 1953.
[18]Leathem, J. G., *Volume and Surface Integrals Used in Physics*, Hafner, New York, 1912.
[19]Kellogg, O. D., *Foundations of Potential Theory*, Dover, New York, 1953.
[20]Mangler, K. W., "Improper Integrals in Theoretical Aerodynamics," Brit. A. R. C., R&M 2424, 1951.
[21]Bisplinghoff, R. L., Ashley, H., and Halfman, R. L., *Aeroelasticity*, Addison-Wesley, Menlo Park, Calif., 1955.
[22]Long, L. N. and Watts, G. A., "A General Theory of Arbitrary Motion Aerodynamics using an Aeroacoustic Approach," AGARD Fluid Dynamics Panel Symposium on Aerodynamics and Acoustics of Propellers, CP-366 Toronto, Oct. 1984 (submitted to *AIAA Journal*).
[23]Jones, R., "The Distribution of Normal Pressures on a Prolate Spheroid, ACR, R&M 1061, 1925.
[24]Van Dyke, M., *Perturbation Methods in Fluid Mechanics*, Parabolic Press, Stanford, Calif., 1975.
[25]Abbott, I. H. and von Doenhoff, A. E., *Theory of Wing Sections*, Dover, New York, 1959.
[26]Gray, R. B., McMahon, H. M., Shenoy, K. R., and Hammer, M. L., "Surface Pressure Measurements at Two Tips of a Model Helicopter Rotor in Hover," NASA CR-3281, 1980.